Lunar Forced Mauna Loa and Atlantic CO_2 Variability

Correspondence to
Harald.Yndestad@ntnu.no

Vol. 2.3 (2022)
pp. 258-274

Harald Yndestad

Norwegian University of Science and Technology,
N-6025, Aalesund, Norway

Abstract

The source of atmospheric CO_2 variations is poorly understood. At Mauna Loa Hawaii, atmospheric CO_2 has been recorded from 1959. This is a short period for a reliable variability signature identification. From the 19th century, atmospheric CO_2 has been recorded in several short periods over the Atlantic Ocean and Europe. A number of these data series are compiled into a single atmospheric Atlantic CO_2 data series from 1820 to 1960. Altogether, this time series covers atmospheric CO_2 records over a total period of 200 years. In this investigation, a wavelet spectrum analysis identifies the signature of Mauna Loa atmospheric CO_2 growth from 1960 to 2020 and Atlantic atmospheric CO_2 for the period 1870 to 1960. The result reveals that the Atlantic CO_2 variability from 1870-1960 coincides with Mauna Loa CO_2 growth variability, global sea surface temperature variability and lunar nodal tide variability. The Atlantic CO_2 signature and global sea surface temperature signature and the have a phase difference of $\pi/2$ (rad), which reveals a sea temperature driven atmospheric CO_2 variation. The CO_2 variability signature coincides with the global sea temperature signature and the lunar nodal signature spectrum. The identified lunar nodal tide spectrum reveals a chain of events from lunar nodal tide variations to global sea surface temperature variations and atmospheric CO_2 variations. A lunar nodal tide spectrum in atmospheric CO_2 growth reveals that CO_2 is not controllable.

Keywords: Mauna Loa atmospheric CO_2 variability; Atlantic atmospheric CO_2 variability; Global Sea surface temperature variability; Lunar nodal tide variability.

Submitted 2022-10-08, Accepted 2022-12-18, https://doi.org/10.53234/scc202212/13.

1. Introduction

1.1 CO_2 at Mauna Loa, Hawaii

There had been a prevailing view of a direct connection between CO_2 and acidity in rivers and groundwater. In 1956, the young polymer chemistry scientist Charles David Keeling, began measuring the concentration of CO_2 in the atmosphere. The results showed that there was no such direct connection. At the same time, he discovered that CO_2 in the atmosphere had its own cycle. The concentration of CO_2 in the atmosphere was lower during the day, when nature absorbed CO_2 in photosynthesis. At sunset, photosynthesis stopped and released CO_2 back into the atmosphere. Keeling had discovered that the local forest breathed in diurnal variations.

Keeling used a new method to record CO_2, based on infrared spectroscopy, to create comparable samples over larger areas. With faster measurements, he was able to detect variations in CO_2 in landscapes and urban areas. CO_2 had large diurnal variations related to local conditions. In hope of finding a stable CO_2 background level, Keeling started monitoring CO_2 at Mount Mauna Loa, Hawaii. It soon turned out that the atmosphere breathed in annual

rhythm and CO_2 also did not have a stable background level. The CO_2 background level increased slightly each year. David Keeling had discovered that concentration of CO_2 in the atmosphere background was growing. This atmospheric CO_2 growth must have a source. The suspicion was accumulation of CO_2 from combustion of fossil fuels, which confirmed the Greenhouse paradigm (Kunzig and Wallace 2008; Keeling et al. 1976; Thoning et al. 1989; Thomas et al. 2016).

1.2 The Greenhouse paradigm

At the beginning of the 19th century, there was a belief in science that large stones in open landscapes were remnants of the flood, known from the Bible. Around 1830, it was discovered that these stones were remnants from an ice age. The discovery of ice ages created speculations about possible causes for these. In 1850, the Irish physicist John Tyndall conducted a laboratory experiment that showed that atmospheric infrared absorption is largely due to carbon dioxide and water vapor. The evidence was that water vapor has a strong effect on the absorption of infrared radiation emitted from the earth's surface. He stressed that the climate would be much colder at night in the absence of the greenhouse effect. This experiment created the idea, that CO_2 enters the atmosphere, and acts as a global climate regulator. He concluded that water vapor is the gas that most strongly absorbs heat radiation in the atmosphere and controls the air temperature (Kunzig and Wallace 2008; Thomas et al. 2016).

The Swedish geologist Arvid Högblom believed that CO_2 from volcanoes created large climate variations and controlled the risk of new ice ages. When volcanoes created a high concentration of CO_2 in the atmosphere, we had a warm climate period, where photosynthesis created more growth in the global ecosystem. The growth of the ecosystem drew CO_2 out of the atmosphere, and into the earth as plant remains. Less CO_2 in the atmosphere led to a gradually colder climate, and eventually a new ice age. Sooner or later, CO_2 emissions came into the atmosphere from volcanoes, which started a new warm climate period. There was a direct connection between CO_2, ecosystems, and ice ages. In the 1890s, the Swedish chemist Svante Arrhenius made calculations which showed that halving CO_2 in the atmosphere led to a global temperature reduction of 4-5 degrees. A doubling of CO_2 will lead to an estimated increase of 5-6 degrees. Arrhenius believed that human CO_2 supply to the atmosphere, had saved us from a new ice age (Kunzig and Wallace 2008; Thomas et al. 2016).

The English railway engineer Gay Stewart Callendar (1898-1964) began studying the relationship between global temperature and CO_2. Based on data from 147 global measuring stations, he was able to show that the global temperature had risen 0.3 degrees C from 1880 to 1930. This corresponds to approximately 0.6 degrees in 100 years. From 1880 to 1930, selected CO_2 measurements had risen by 6 %. In 1938 he wrote an article in which he pointed out that humans have already contributed to half of the CO_2 growth in the atmosphere. Humans had increased the global temperature by 0.3 degrees per century. This had led to a more pleasant climate in the northern hemisphere, following the cold climate of the 19th century, and saved the planet. Callendar developed a model that showed a linear relationship between man-made CO_2 and global temperature. This linear relation between CO_2 and global temperature, introduced the idea of climate as a closed system on Earth, which ignores natural variations (Kunzig and Wallace 2008; Thomas et al. 2016; Anderson et al. 2016).

1.3 Ocean surface carbon system

The young Japanese student Taro Takahashi studied to become a mining engineer, like his father and grandfather. After his studies, he was tempted to participate in the study of the Atlantic Ocean to record CO_2 in the atmosphere. This was the start of a 60-year research project. Atmospheric CO_2 growth had raised questions about the impact on the ocean's carbon system. In the 1970s, Taro Takahashi began measuring CO_2 over oceans. He discovered that oceans breathed CO_2 over diurnal variations, between cold and warm ocean variations and between

climate variations. Warm sea regions released CO_2 from the sea area and increased the concentration of the CO_2 atmosphere. In the cold sea areas between Iceland and Greenland, CO_2 was absorbed from the atmosphere by the sea. Takahashi had discovered that a higher sea temperature released more CO_2 into the atmosphere. CO_2 in the atmosphere was climate-driven, with air currents carrying CO_2 between different regional ocean areas. However, climate-driven CO_2 is not the same as a CO_2-driven climate. He discovered that CO_2 over the oceans acts as a dynamic system associated with marine ecosystems, cold and warm ocean currents, with circulation times from years to thousands of years. At the same time CO_2 in the atmosphere is a distribution system between sea areas, land, and ecosystems, in short and long circulation periods (Kunzig and Wallace 2008; Tansinez et al. 1990; Krajick 2019; Gruber et al. 2009).

1.4 Atlantic CO_2 variations 1826-1960

Ernst-Georg Beck was a German teacher of biology, of the old school, at the Merian Technical Grammar School in Freiburg and co-founder of the European Institute for Climate and Energy (EIKE). Beck began asking critical questions about the recorded CO_2 time-series at the Hawaiian volcano Mauna Loa. He considered warming of the Earth's atmosphere, due to an increase in CO_2 in the atmosphere, as impossible. At the same time, he believed that the CO_2 records at Mauna Loa could not be extrapolated linearly back to the 19th century, as has been done at Mauna Loa Observatory (Keeling et al. 1976).

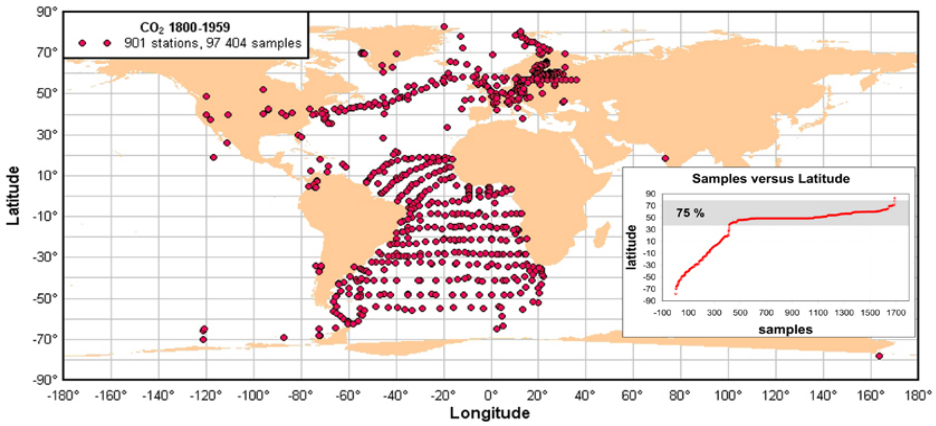

Figure 1: 901 sampling stations of direct measured CO_2 near ground 1800-1960 (Beck 2007).

Estimates of atmospheric CO_2 did not start with David Keeling and Takahashi. Chemical estimates of atmospheric CO_2 have been recorded since beginning of the 19th century. Callendar used previous CO_2 records from 1880 to 1930 to estimate a relation between global CO_2 and global warming. Seventy years later, Ernst Beck began estimating a new CO_2 time series based on previously published CO_2 time-series, most likely, including some of the same data, as used by Callendar (Anderson et al. 2016). In this extensive and highly impressive work, Beck conducted a review of approximately 100.000 CO_2 records from 901 recording stations (Fig. 1).

The result was published in 2007 (Beck 2007). In the Abstract Beck writes:" More *than 90,000 accurate chemical analyses of CO_2 in air since 1812 are summarized. The historic chemical data reveal that changes in CO_2 track changes in temperature, and therefore climate in contrast to the simple, monotonically increasing CO_2 trend depicted in the post-1990 literature on climate-change. Since 1812, the CO_2 concentration in northern hemispheric air has fluctuated exhibiting three high level maxima around 1825, 1857 and 1942 the latter showing more than 400 ppm."* This result questioned the Greenhouse paradigm in several ways. CO_2 was not accumulated in the atmosphere. There were large CO_2 fluctuations between 1826 and 1960.

Ralph F. Keeling, (son of David Keeling) responded. "*If Beck's contentions were true, they would overthrow 50 years of scientific advance and discovery. Unfortunately for Beck—as well as for humanity—the claims don't stand up. A historic perspective is useful. The modern era of CO_2 measurements effectively began with work by C. D. Keeling while he was a postdoc at the California Institute of Technology in the mid 1950's. It should be added that Beck's analysis also runs afoul of a basic accounting problem. Beck's 11-year averages show large swings, including an increase from 310 to 420 ppm between 1920 and 1945 (Beck's Fig. 11). To drive an increase of this magnitude globally requires the release of 233 billion metric tons of carbon to the atmosphere. The amount is equivalent to more than a third of all the carbon contained in land plants globally. Other CO_2 swings noted by Beck require similarly large releases or uptakes. To make a credible case, Beck needed to offer evidence for losses or gains of carbon of this magnitude from somewhere. He offered none. »* (Keeling 2007).

The time series from Beck showed that CO_2 had an unexpectedly strong growth between 1920 and 1945. Beck had not explained this CO_2 growth. A temporary CO_2 growth, which did not agree with the idea of accumulated CO_2 in the atmosphere, from combustion of fossil fuels. This led to questions about the credibility of the Atlantic CO_2 time series from Beck.

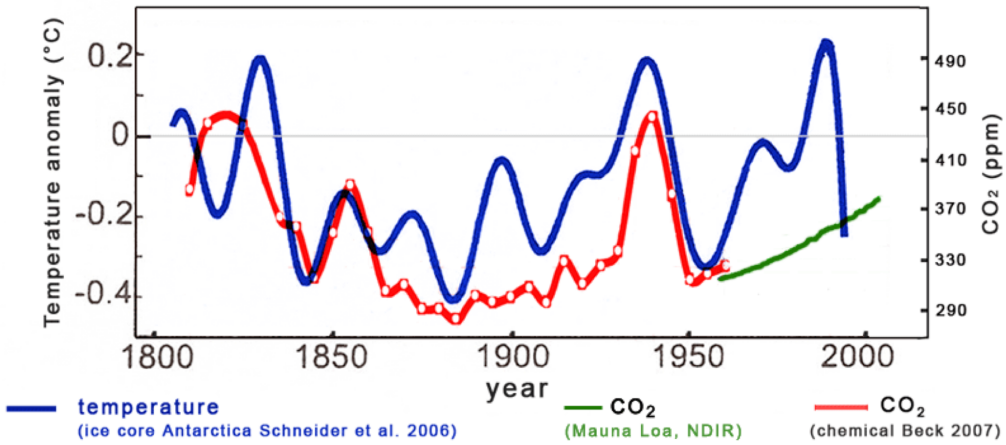

Figure 2: Atlantic CO_2 (1812-1961), Antarctic temperature (1812-1990), Mauna Loa atmospheric CO_2 (1960-2005) (Beck 2008b).

Beck responded to the criticism from Ralph Keeling (2007) with a discussion article in 2008 (Beck E. G. 2008b). Here he presents a figure that shows a reasonably good agreement between CO_2 and temperature changes in Antarctica from ice core samples (Fig. 2). The Mauna Loa CO_2 showed a slow growth, without large fluctuations. This close relation between Atlantic CO_2 and Antarctic temperature estimates was published in December 2008.

In 2008 a wavelet spectrum analysis of the North Atlantic water (NAW) inflow from 1900 to 2007 (Yndestad et al. 2008) was published. This paper revealed a close relation between (NAW) and CO_2 growth between 1930 and 1950. In this paper Beck found the explanation for the unexpected CO_2 growth in the atmosphere during this period. Temperature variations in Atlantic water released large amounts of CO_2 into the atmosphere. The unknown source of CO_2 growth coincided with temperature variations in the North Atlantic Ocean. In 2009 Beck started to work on an updated manuscript. In this manuscript, he adds a review of estimate variations, and selected the most reliable data and explained the CO_2 growth from 1920 to 1945.

The manuscript was submitted for publication in August 2010 (Beck February 2010). In the discussion Beck writes: *"Using a Savitzky-Golay smoothed curve with a higher moving window*

width of 7 to correct problems around 1880 and 1930. Observed a periodic cycling with maxima at: 1836: 343,9 ppm; 1857: 334,2 ppm; =1878: 309,7 ppm; 1896: 312 ppm; 1915: 320,7 ppm; 1941: 371,4 ppm. The average period is 21 years (21, 21, 18, 19, 26 years).

The sharp drop in 1922 and the changing period length at those times points to phase change in the time series supports the findings of Yndestad in the NAW (Northern Atlantic water temperature) [Yndestad et al. 2008], evidence for the lunar nodal cycle and its harmonics as the controlling forces behind the northern and Arctic climate"…"Since 1870 two periods of about 60-70 years (1870-1940) and 1949 -2009 can be observed with such a slowly rise of the CO_2 levels to a maximum level of about + 70 ppm in about 1943 and today. The overall rising CO_2 levels since 1870 to today has been also supported by the reconstructed ice core data despite of its much worse resolution compared to the presented data (see fig. 25). The maxima around 1860, 1940 contrast with the published literature. They can be described by an about 70-80-year cycle". Beck died of cancer in September 2010. The manuscript was rejected for publication on November 15, 2010. The last reviewer comment was "*I must categorically advise rejection of this paper without possibility of resubmission or revision"* (Beck 2007; Harro A.J. Meiyer. 2007; Keeling R.F. 2007; Beck E. G. 2008a; Beck E. G. 2008b; Massen, Francis and Beck E. G. 2011; Keeling R.F. 2007; Beck E. G. February 2010; Ernst-Georg Beck's scientific contributions. ResearchGate).

Taro Takahashi and Ernst Beck argued that CO_2 variations in the atmosphere were controlled by sea surface temperature. This can be verified by computing the variability signature atmospheric CO_2 and global sea surface temperature. In 2008, a wavelet spectrum analysis of North Atlantic Water from the year 1900 was published (Yndestad et al. 2008). The analysis confirmed a coincidence between Atlantic CO_2 and sea surface temperature variations in the period 1930-1960. This analysis confirmed the last part of the data series for Beck, and it explained the 1930-1950 CO_2 bubble. In 2022 there was published a wavelet spectrum analysis global sea surface temperature variability from 1850 to 2020. The wavelet spectrum revealed a coincidence to the lunar nodal tide spectrum signature (Yndestad 2022). The implication of a lunar nodal spectrum in global sea temperature variations is that the sea temperature variations are controlled by the lunar nodal tide, which is not controllable. This study investigates the Mauna Loa CO_2 variability signature from 1959 and Atlantic CO_2 variability signature from 1850 to 1960.

2. Materials and methods

2.1 Materials

The Mauna Loa CO_2 time series, shown on Fig. 3 covers the period 1958 to 2021, representing the longest continuous recording of direct atmospheric CO_2 measurements. Data are recorded at an altitude of 3400 m in the northern subtropics, which is not identical to the global average CO_2 concentration at the surface. The time series is monitored by the NOAA Global Monitoring Laboratory (https://gml.noaa.gov/ccgg/trends/data.html). The red graph shows annual seasonal variations around an average annual CO_2 growth that apparently has an exponential growth (Fig. 3). The source of annual seasonal variations is believed to be seasonal variations from photosynthesis in nature. The overall increase in CO_2 from 1958 has been associated with accumulation of CO_2 from fossil fuels. The Atlantic CO_2 time series is based on Beck (2022; https://doi.org/10.53234/scc202206/20).This time series covers records from the Atlantic Ocean and Northern Europe. The time series covers the period 1826 to 1960, estimated from selected 97 404 selected samples from 901 stations compiled in 87 data files (Beck 2022). The sea surface temperature (SST) time series (HadSST3) consists of anomalies on a 5°-by-5° global grid and is published by the Climatic Research Unit. The SST signature is computed in (Yndestad 2022). (For SST, see https://www.metoffice.gov.uk/hadobs/hadsst3/).

2.2 Methods

A wavelet analysis provides temporal, cycle period and cycle phase information in time series. The wavelet spectrum transform is based on a correlation between a time series and a bell-shaped wavelet pulse s(t) that moves along the time axis of the time series t = [first…last]. You then get a large numeric value where you have a match between the wavelet pulse and periodic changes in the time series. By changing the pulse width, one can identify all the periodic changes in the time series. Cycle periods and cycle phase relations are identified in the wavelet spectra by the continuous wavelet transform:

$$W_{a,b}(t) = \frac{1}{\sqrt{a}} \int_R \; x(t)\, \Psi\left(\frac{t-b}{a}\right) dt \tag{1}$$

where x(t) is the analyzed temperature time series after being scaled to zero mean value and scaled by variance. In the present case, Ψ() is a coif3 wavelet impulse function. $W_{a,b}(t)$ is a set of wavelet cycles, b is the translation in time, and a is the time-scaling parameter in the wavelet transformation (Daubechies 1992; MATLAB, 2020), which is in this case performed as a discrete wavelet transform. In this analysis, the time translation b = 0, and the computed wavelet transform, $W_a(t)$, represents a moving correlation between x(t) and the impulse function Ψ() over the entire time-series x(t). The moving correlated wavelets, s(t), are collected into a wavelet spectrum, W(s, t), for t = [first…last] (yr.) and s = [1…(last-first)/2] (yr.), to comply with the sampling theorem. Stationary cycles are identified by computing the autocorrelation of the wavelet spectrum W(s, t), as follows:

$$WA(R(s), m) = E[W(s, t)W(s, t + m)], \tag{2}$$

where WA(R, T) represents a set of maximum correlation values R = [max 1…max n] with the dominant cycles T = [T1…Tn] (yr.).

2.3 Scientific approach

A CO_2 time series has a spectrum signature: $S_{co2}(T_{co2}, F_{co2})$, where T_{co2} represents a set of stationary CO_2 cycle periods and F_{co2} represents CO_2 cycle phase relations (min/max). Global Sea Surface Temperature (SST) has a spectrum signature $S_{sst}(T_{sst}, F_{sst})$, where T_{sst} represents a set stationary SST cycle periods and F_{sst} represents a set of cycle phase relations. The CO_2 spectrum signature and the SST spectrum signature have a relation:

$$S_{co2}(T_{co2}, F_{co2}) = S_{sst}(T_{sst,} F_{sst}) + S_{err}(T_{err}, F_{err}), \tag{3}$$

where $S_{err}(T_{err}, F_{err})$ represents a spectrum from an unknown source. A CO_2 signature $S_{co2}(T_{co2}, F_{co2})$ coincides with the Sea Surface Temperature (SST) signature, $S_{sst}(T_{sst}, F_{sst})$, if: $S_{co2}(T_{co2}, F_{co2}) = S_{sst}(T_{sst}, F_{sst})$. The CO_2 signature, $S_{co2}(T_{co2}, F_{co2})$, has a π/2 (rad) phase lag if: $S_{co2}(T_{co2}, F_{co2}) = S_{sst}(T_{sst}, F_{sst} + T_{sst}/4)$.

3. Results

3.1. Mauna Loa CO_2 variability 1959-2021

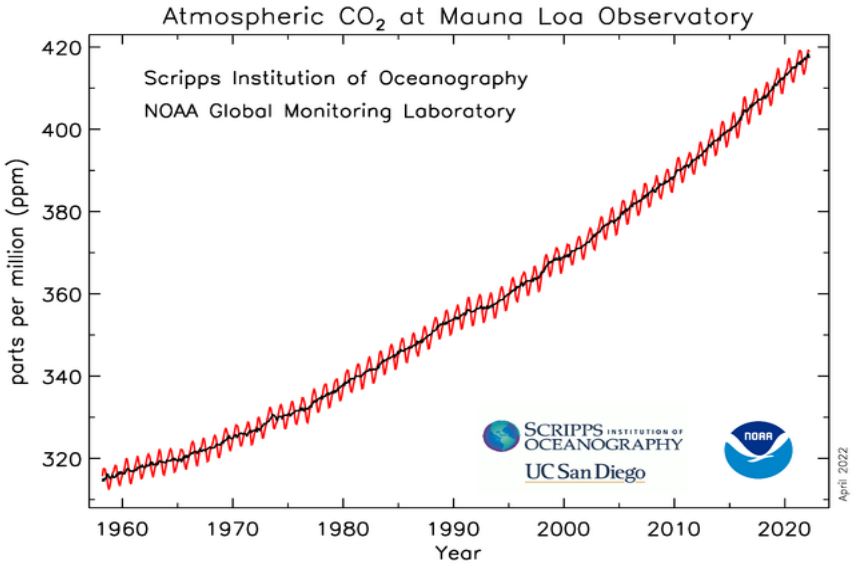

Figure 3: Mauna Loa, Hawaii, recorded atmospheric CO_2 (ppm) for the years t = 1959...2021.

Records of CO_2 from 1959 to 2021 at Mauna Loa, Hawaii is shown on Fig. 3. The CO_2 level appears to have an exponential growth. This exponential growth must have a source. Possible sources are emission from fossil fuels and net outgassing of CO_2 from the oceans. The CO_2 time series covers a period of 62 years. In this short time-period, CO_2 has grown by 100 ppm and global temperature has grown by 0.6 degrees C. The CO_2 growth at Mauna Loa is time-variant. The growth has a minimum in the cold climate period during the 1960´s and a maximum growth in the warm climate period close to 2020. The time-variant growth rate signature may reveal the source of the Mauna Loa CO_2 variations.

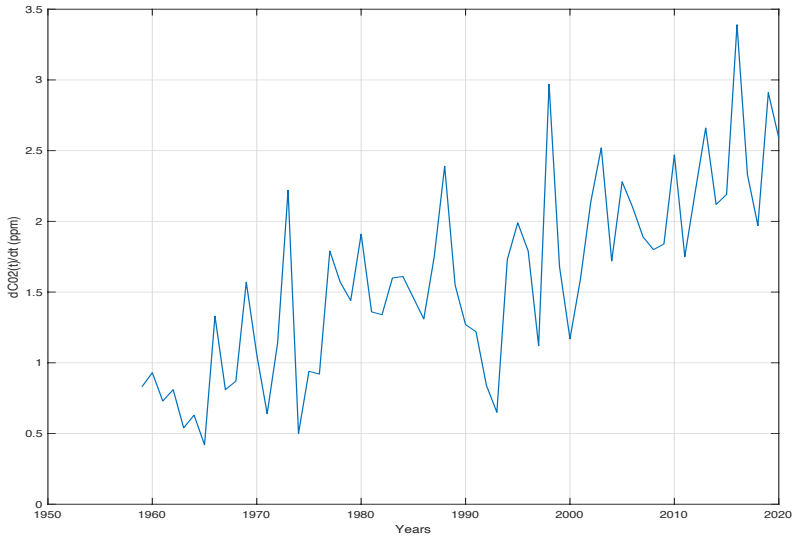

Figure 4: Annual Mauna Loa CO_2 growth rate, dCO_2/dt, for the years t = [1959...2020].

The Mauna Loa CO_2 time series has an annual growth rate $dCO_2(t)/dt = (CO_2(t) - CO_2(t-1))/dt$, for the period t = [1959, 1960...2020] (Fig. 4). It appears from Fig. 4 that the CO_2 growth rate,

$dCO_2(t)/dt$, began to increase from about 1965 and reached a maximum close to 2016 The growth rate, $dCO_2(t)/dt$, has a minimum close to the cold period in the 1960s and stabilized to a maximum when global sea temperature has a maximum from about the year 2010 (Yndestad 2022). At the same time, the growth rate (Fig. 4) has some large fluctuations.

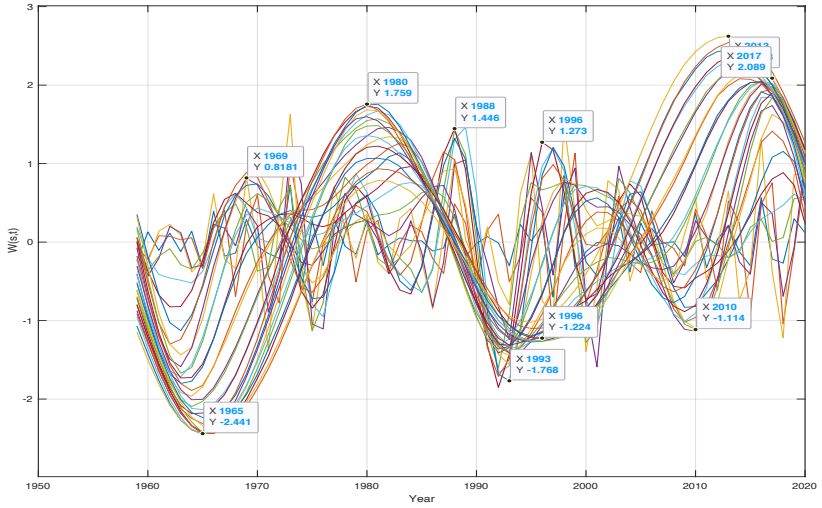

Figure 5: Wavelet spectrum, $W_{co2\text{-}m}(s, t)$, from Mauna Loa in CO2 growth (dCO_2/dt) for t = [1959…2021] and s = [1…30]. The wavelet spectrum reveals cycle periods in annual Mauna Loa CO2 growth rate (Fig. 4).

The fluctuation source is revealed by computing the signature in the wavelet spectrum [Eq.1]. The Mauna Loa time series has 62 samples, which may represent periods up to 31 years. Fig. 5 shows the computed wavelet spectrum $W_{co2\text{-}m}(s, t)$ of Mauna Loa CO_2 growth rate $dCO_2(t)/dt$ when t = [1959…2021] and s = [1…30]. The computed wavelet spectrum has min/max variations for: $W_{co2\text{-}m}$(s = min/max, t) = [(-1.64, 1965), (-0.0, 1973), (1.8, 1980), (+0.0, 1988), (-1.2. 1995), (-0, 2004), (2.5, 2013)] at intervals of [8, 7, 8, 7, 9, 9] (yr.), which has a mean cycle period of $T_{co2\text{-}m}$ = 32 years.

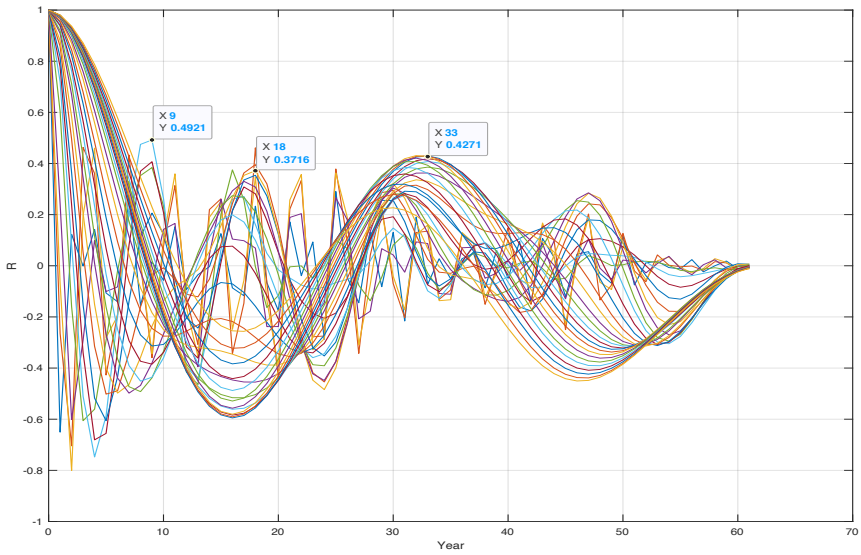

Figure 6: Autocorrelations, $WA_{co2\text{-}m}(R(s), m)$, of Mauna Loa CO_2 wavelet spectrum, $W_{co2\text{-}m}(s, t)$, for s = [1…60] and m = [1…60].

Stationary periods in the wavelet spectrum, $W_{co2\text{-}m}(s, t)$, (Fig. 6) are estimated by computing the autocorrelation of all wavelets in the wavelength spectrum $W_{co2\text{-}m}(s, t)$ [Eq. 2]. The computed wavelet autocorrelation spectrum, $W_{aco2\text{-}m}(R(s), m)$, for the wavelet spectrum: $W_{co2\text{-}m}(s, t)$, have maximum correlations at: $WA_{co2\text{-}m}(R(max), T_{co2\text{-}m}) = [(0.5, 3), (0.5, 9), (0.4, 18), (0.42, 33)]$ (Fig. 6), where the maximum correlation $R(max) = [0.5, 0.5, 0.4]$ to the stationary periods: $T_{co2\text{-}m} = [3, 9, 18, 33]$ (yr.).

CO_2 and SST signature coincidence

Global Sea Surface temperature (SST) has a coincidence to the lunar nodal spectrum: $T_{sst} = [1/3, 1, 2, 3]18.61/2 = [3.1, 9.3, 18.6, 27.9]$ (yr.) (Yndestad 2022). The coincidence difference between identified stationary CO_2 growth rate periods, $T_{co2\text{-}m}$, and lunar forced SST periods, T_{sst}, is: $[T_{co2\text{-}m} - T_{sst}] = [0, 0, 0, 5]$ (yr.), which reveals a direct coincidence between identified CO_2 growth rate periods and deterministic lunar nodal periods. The global sea surface temperature wavelet spectrum, $W_{sst}(s, t)$, has computed phase shifts at the years: $W_{sst}(s = min/max/0, t) = [(+0, 1960), (-3.9, 1977), (-0, 1993), (5.1, 2008)]$ (Yndestad 2022).

The phase difference: $[W_{sst}(s = min/max/0, t) - W_{co2\text{-}m}(s = min/max/0, t)] = [(+0, 1960), (-3.9, 1977), (-0, 1993), (5.1, 2008)] - [(-1.65, 1964), (-0\ 1973), (-1.2, 1995), (-0, 2004)] = [4, 4, 2, 4]$ years, reveals that CO_2 growth rate, $dCO_2(t)/dt$, has a $\pi/2$ (rad) phase lag from global sea temperature variations. Warmer sea surface temperature causes more rapidly accumulation of CO_2 in the atmosphere.

3.2. Atlantic CO_2 variability 1826-1960

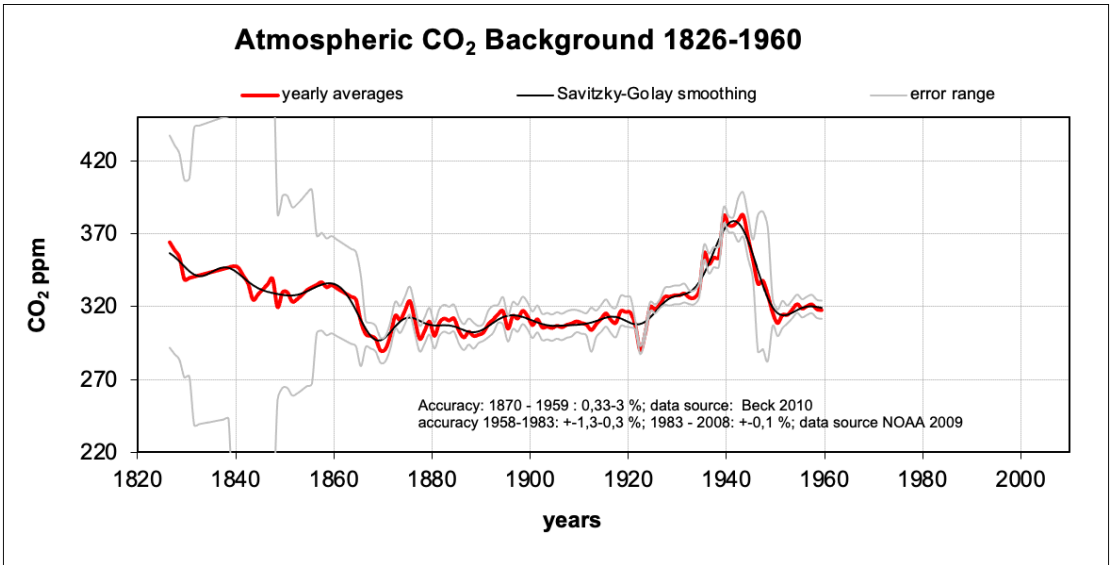

Figure 7: Beck CO_2 time series 1826-1960, (Beck February 2010, Beck 2022, Supplemental data No. 2. https://doi.org/10.53234/scc202206/20)

Estimated CO_2 for the period 1826 to 1960 is shown on Fig. 7. About 75 % of the samples were collected between latitudes of 40 and 80 N, about 50 % over sea surface or from the sea at coasts (Beck February 2010; Beck 2022). The data series is estimated from more than 200 000 single samples in about 400 historical papers from 1800 to 1960 (Beck February 2010). The Mauna Loa time series (Fig. 3) has an exponential growth from 1960. The Atlantic CO_2 time series starting in 1826 is different. The CO_2 levels are dropping from 1826 to a minimum around 1870, continued to grow from 1930 to a temporary maximum around 1940 and a new temporary minimum in 1950. The CO_2 growth in this period was questioned by Ralph Keeling (Keeling 2007). The CO_2 estimates are not accurate from 1826 to 1870. From 1870 the accuracy is

estimated to 3%. The total time series covers a total period of 134 years, which may represent a period up to 67 years.

3.3 Atlantic CO_2 wavelet spectrum from 1826 to 1960

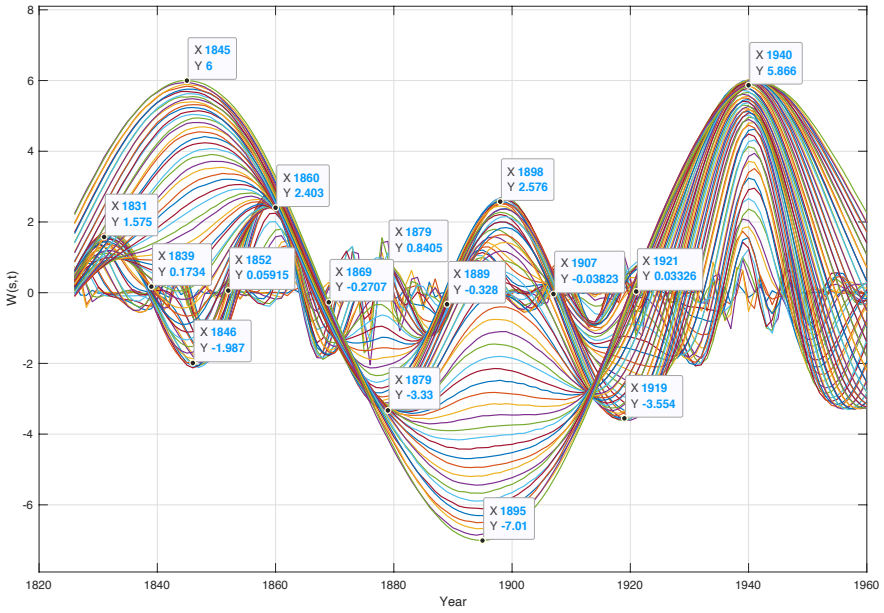

Figure 8: Wavelet spectrum, $W_{co2\text{-}a}(s, t)$, of Atlantic surface CO_2 (Beck E.G. February 2010) for $s = [1...70]$ in the years $t = [1826...1960]$.

The computed wavelet spectrum of Atlantic surface CO_2 (Beck E.G. February 2010) (Fig. 8) for s = [1...70] in the years t = [1826...1960]. The long envelope period in the wavelet spectrum (Fig. 8) has minima, maxima, and phase shifts at the years: $W_{co2\text{-}a}$(s = min/max/0, t) = [(6.0, 1845), (+0.0, 1868), (-7.0, 1895), (-0.0, 1921), (5.8, 1940)] in a total period of 95 years. The next part of the wavelet spectrum (Fig. 8) has phase shifts at: $W_{co2\text{-}a}$(s = min/max/0, t) = [(1.6, 1831), (+0, 1839), (-2.0, 1846), (-0.0, 1852), (2.4, 1860), (+0.0, 1868), (-3.3, 1879), (-0.0, 1889), (2.6, 1898), (+0.0, 1907), (-3.5, 1919), (-0.0, 1929), (2.5, 1940)], in a mean period of 36 years. The estimated 36-year wavelet cycle, $W_{co2\text{-}a}$(s = 36, t), coincides with lunar nodal periods of 2*18.6 = 37.2 years. The 95-year wavelet, $W_{co2\text{-}a}$(s = 95, t), coincides with a lunar nodal period of: 5*18.6 = 93.0 years. The CO_2 growth between 1930 and 1950 coincides with a constructive interference between the stationary lunar nodal cycles of 37.2 and 93.0 years. In this period the lunar nodal cycle has a direct relation to global sea temperature variations.

Computed upcoming minima and maxima

A stationary lunar forced 2*18.6 = 37.2-year period is expected to have upcoming minima, maxima and phase shifts at the years: $W_{co2\text{-}a}$(s = 37.2, min/max/0, t) = [(min, 1811), (max, 1829), (min, 1848), (max, 1866), (min, 1884), (max,1903), (min, 1922), (max, 1940), (min, 1959), (-0, 1968), (max, 1977), (+0, 1986), (min, 1996)…(-0, 2005), (max, 2014), (+0, 2023), (min, 2033)]. The stationary 93.0-year lunar forced period is expected to have phase shifts at the years: $W_{co2\text{-}a}$(s = 93.0, min/max/0, t) = [(6.0, 1845), (+0.0, 1868), (-7.0, 1895), (-0.0, 1921), (5.8, 1940), (+0, 1963), (min, 1986), (-0, 2009), (max, 2033), (+0, 2056)]. The stationary dominant periods have destructive interference from 1826-1930, constructive positive interference from 1930-1950, destructive interference from 1950-1987 and growth from 1987-2022. The computed CO_2 growth from 1987-2022, coincides with global sea surface temperature growth (Yndestad 2022) and CO_2 growth at Mauna Loa (Fig. 4).

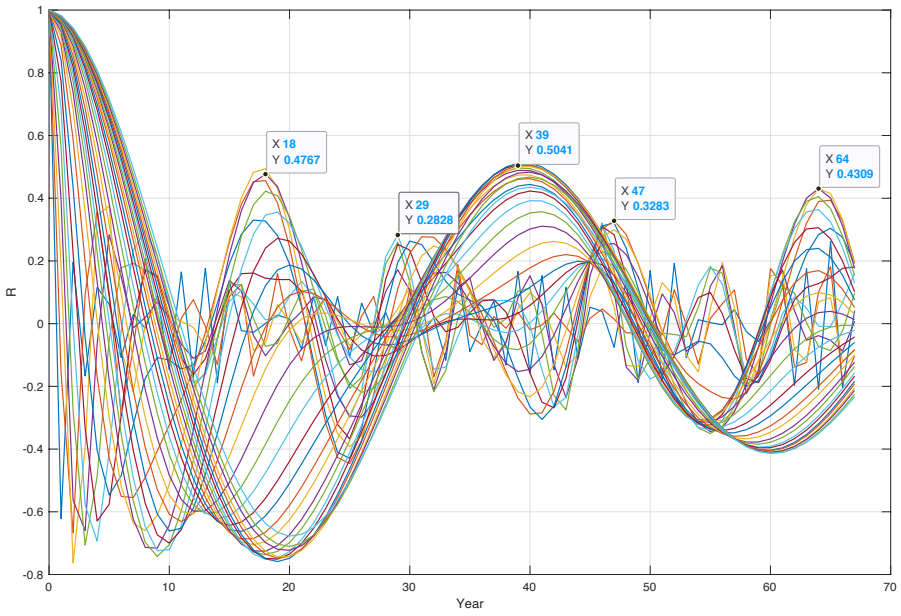

Figure 9. Autocorrelations, $WA_{co2\text{-}a}(R(s), m)$, of wavelet spectrum, $W_{co2\text{-}a}(s, t)$, for annual background growth in CO_2 (Beck 2010) for s = [1...70] and m = [1...67].

Stationary CO_2 periods in the wavelet spectrum, $W_{co2\text{-}a}(s, t)$, (Fig. 8) are estimated by computing the autocorrelation of all wavelets in the wavelet spectrum. The computed autocorrelations, $WA_{co2\text{-}a}(R, m)$ (Fig. 9), for the wavelet spectrum, $W_{co2\text{-}a}(s, t)$, have maximum correlations in the following periods: $WA_{co2\text{-}a}(R(max), T_{co2\text{-}a}) = [(0.3, 9), (0.47, 18), (0.26, 29), (0.5, 39), (0.3, 47), (0.4, 64)]$, which represents the correlations: R = [0.3, 0.47, 0.26, 0.50, 0.3, 0.4] to the periods: $T_{co2\text{-}a}$ = [9, 18, 29, 39, 47, 64] (yr.). Lunar nodal forced SST cycles have a spectrum: T_{sst} = [1, 2, 3, 4, 5, 7]18.6/2 = [9, 18.6, 27.9, 37.2, 46.5, 65.1] (yr.) (Yndestad 2022). The coincidence difference between estimated $T_{co2\text{-}a}$ cycle periods and lunar nodal forced SST cycles are: $[T_{co2\text{-}a} - T_{sst}]$ = [0, 0, 2, 0, 0, 1] (yr.), or a mean difference of 0.5 years.

3.4 Atlantic CO_2 and SST signature coincidences

Global sea surface temperature variability has a stationary period spectrum: T_{sst} = [18, 29, 39, 64, 74] (yr.), in coincides with the lunar nodal spectrum T_{ln}. The coincidence difference between stationary global sea surface periods, T_{sst}, and Atlantic CO_2 periods is: $[T_{sst} - T_{co2\text{-}a}]$ = [0, 0, 0, 0, 19] (yr.). The 19-year difference indicates that the average error from 1826 to 1870 has introduced a period shift from a 74-year period to a 93-year period in estimated Atlantic CO_2 variability. The SST has phase shifts at the years: $W_{sst}(s = min/max/0, t) = [(+0, 1897), (+0, 1960), (-0, 1993), (5.1, 2008)]$ (Yndestad 2022; Yndestad et al. 2008). The stationary 36-year Atlantic CO_2 periods has a minimum and maximum at: $W_{co2\text{-}a}(s = 36, t) = [(2.6, 1898), (-3.6, 1960)]$, which reveals a $\pi/2$ (rad) phase lag from global sea surface variations to Atlantic CO_2 variations. The extended stationary CO_2 period $W_{co2\text{-}a}(s = 37.2, t)$ has phase shifts at the years; $W_{co2\text{-}a}(s = 37.2, min/max/0, t) = [(max, 1940), (+0, 1949), (min, 1959), (-0, 1968), (max, 1977), (+0, 1987), (min, 1996), (-0, 2005), (max, 2015)]$. The phase difference between the lunar driven SST period and the lunar driven CO_2 period is: $[W_{sst}(s = min/max/0, t) - W_{co2\text{-}a}(s = min/max/0 - \pi/2 (rad), t)] = [1, 1, 3, 3]$ (yr.), which has a mean difference of only 2 years. Stationary Atlantic CO_2 periods has a $\pi/2$ (rad) phase lag from stationary Global Sea Surface periods from 1870 to 2020. Atlantic CO_2 growth rate has a maximum when SST has a maximum amplitude.

3.5 Mauna Loa CO_2 coincidences

The Mauna Loa CO_2 growth rate, dCO_2/dt, has period phase shifts at: $W_{co2\text{-}m}(s = min/max/0, t)$ = [(-1.64, 1965), (-0.0, 1973), (1.8, 1980), (+0.0, 1988), (-1.2, 1995), (-0, 2004), (2.5, 2013)]. The Atlantic 37.2-year CO_2 period has phase shifts at the years: $W_{Co2\text{-}a}(s = 37.2, min/max/0, t)$ = [(max, 1940), (+0, 1949), (min, 1959), (-0, 1968), (max, 1977), (+0, 1987), (min, 1996), (-0, 2005), (max, 2015)]. The phase difference between Mauna Loa CO_2 growth rate and extended Atlantic CO_2 periods is: $[W_{C02\text{-}m}(s = min/max/0, t) - W_{co2\text{-}a}(s = 37.2, min/max/0, t)]$ = [3, 4, 1, 1, 2] (yr.), which has a mean difference of only 2.2 years.

4. Discussion

4.1 Chemical-based CO_2 recordings

Monitoring atmospheric CO_2 started early in the 1800's by a chemical-based method. This was probably an expensive and time-consuming method that required special knowledge. Beck (February 2010) claimed that the chemical-based method was accurate, where error deviation was less than 3%. It looks like it took a few years before chemical monitoring of atmospheric CO_2 was established according to a unified best practice.

Callendar created a CO_2 time series from 1880 to 1932 based on published CO_2 measurements from different parts of the globe. The selected records were limited to publications he trusted (Thomas et al. 2016). When Beck developed his Atlantic CO_2 time series, he selected previous publications from 1826 to 1960. In the manuscript Beck (February 2010), it appears that Beck rejected some CO_2 publications he did not trust. In retrospect, it has been questioned why some early publications were rejected. Beck calculated uncertainty for each individual year (Fig. 7). This uncertainty is related to variations around a mean estimate. It appears from the figure that the time series has large variations from 1826 to 1870. In the period 1870 to 1960, the variation is about 3%. These variations indicates that the time series is reliable from 1870 to 1960.

4.2 Mauna Loa CO_2 recordings

The Mauna Loa CO_2 records from 1959 were based on infrared spectrometry. This method is obviously a faster, cheaper, and more stable method than records from chemical-registrations. Whether this was a more accurate measurement method is however unclear. Mauna Loa CO_2 records from 1959 became the new standard for recording atmospheric CO_2. In 2009, Ernst Beck came up with an unknown CO_2 atmospheric time series. A time series based on 100,000 CO_2 atmosphere records from 1826 until 1960. Beck points out that Keeling did not have CO_2 data before 1959. He also questions the Greenhouse effect and claims that more heat must be added to release more CO_2 into the atmosphere. Humlum et al. (2013) published an estimated 11–12-month phase lag from global sea surface temperature variations to atmospheric CO_2 variations (Humlum et al. 2013). This estimate supports a temperature-driven CO_2 variation.

The Mauna Loa CO_2 time series from Keeling and the Atlantic CO_2 time series from Beck are the only known long continuous CO_2 atmosphere records. This study therefore is of utmost importance for identifying the relation between CO_2 variability and climate variability. The challenge is that the time series are recorded by different methods, at different geographical positions on Earth. The results from this study have revealed that the time series are not really that different. Variations in CO_2 at Mauna Loa CO_2 and variations in Atlantic CO_2 have the same signature which reveals a variability that has the same source.

Taro Takahashi's records showed that CO_2 had large variations over sea areas on the globe. Atmospheric CO_2 is growing from the sea close to the warm equator and absorbed into the sea in cold Arctic areas. Atlantic CO_2 and Mauna Loa CO_2 looks different because the sea temperature increased in the period 1975 to 2000. Atlantic CO_2 captures regional variations more strongly than recorded CO_2 at an altitude of 3000 meters. Now the NOAA Global

Monitoring Laboratory also confirms that records of CO_2 on Mauna Loa are not the same as global CO_2.

4.3 The Mauna Lua CO_2 signature 1960-2020

This study investigates the coincidence between Mauna Loa CO_2 growth and Atlantic CO_2 density. The wavelet spectrum of CO_2 growth at Mauna Loa coincides with the signature of global ocean surface temperature and the lunar nodal tide signature (Table 1). This coincidence reveals a direct relationship between Mauna Loa CO_2 variability, global surface temperature variability and the lunar nodal tide. CO_2 growth variations at Mauna Loa, have a $\pi/2$ (rad) phase lag from global temperature variations. The phase lag reveals that higher global surface temperatures in the ocean, leads to higher speed in outflow of CO_2 from oceans and into the atmosphere. Variations in the global sea temperature, thus causes CO_2 variations in the atmosphere. The exponential CO_2 growth at Mauna Loa, is caused by global warming from 1975 to 2020. The signature of CO_2 growth also coincides with the signature of the lunar nodal tide. This signature has the periods of T_{ln} = [1/3, 1, 2, 3]18.61/2 years. The lunar nodal time has a spectrum of deterministic periods up to 446 years (Yndestad 2022). When the CO_2 signature coincides with the global sea surface temperature signature and the lunar nodal tide signature, it reveals that CO_2 growth at Mauna Loa is not controllable.

4.4 The Atlantic CO_2 signatures 1870-1960

The wavelet spectrum of Atlantic CO_2 from 1870 to 1960 confirms a direct connection between Atlantic CO_2, global sea surface temperature variations and the lunar nodal tide. The signature of Atlantic CO_2 has dominant lunar node periods of: $T_{co2\text{-}a}$ = [1, 2, 4]18.6 years. Atlantic CO_2 variability is controlled by the global ocean surface temperature variability and lunar nodal tide spectrum. The global sea surface temperature signature and the Atlantic CO_2 signature have a phase difference of $\pi/2$ (rad). This phase difference confirms that a maximum sea temperature, leads to a maximum speed in CO_2 outflow from the sea and into the Earth´s atmosphere. Variations in Atlantic CO_2 from 1870 to 1960 coincide with variations in Mauna Loa CO_2 from 1960. This coincidence confirms that both CO_2 time series are controlled by the same source.

Ralph Keeling questioned the CO_2 growth from 1930 to 1950. The wavelet spectrum analysis reveals that this growth coincides with global ocean surface temperature variations controlled by constructive interference between the 2*18.6 = 37.2 years lunar forced SST period and the 4*18.6 = 74.4 years lunar forced SST period. A continuation of the temperature period of 37.2 years, from 1940 to 2020, reveals that changes in Atlantic CO_2 and Mauna Loa CO_2 have the same period and phase relations. The phase difference is only 2 years. This close relation confirms that Atlantic CO_2 variations and Mauna Loa CO_2 variations have the same source.

The lunar nodal signature in sea surface temperature variations, is controlled by vertical mixing in oceans. Cold bottom water is mixed with surface water heated by the sun. The lunar nodal tide is a standing wave that has maximum amplitude at equator and the pole. The lunar tide thus introduces its signature in sea surface temperature variability. This vertical mixing in the oceans, may be a possible source of releasing more CO_2 from deep water into the atmosphere. Global sea surface temperature has an identified lunar nodal powered spectrum up to 446 years. Sola-forced periods influences the long sea temperature growth from 1896 to 2020 (Yndestad 2022). In this study the two CO_2 data series are too short to identify the long solar-forced period.

A study of glaciological characteristics of the Antarctic Ice Core (Ahn et al. 2012), identified a higher CO_2 density level in the warm climate period 1000-1200 and a lower CO_2 level in the cold period 1450 to 1800. This confirms that CO_2 in the atmosphere follows long-term global temperature variations. Global sea temperature is expected to continue to grow steadily until about 2025-2030. Thereafter, a new cooling period is expected in the future, to a deep minimum of approximately the year 2070 (Yndestad 2022). This means that we may expect that an accelerating CO_2 growth will continue towards the year 2030. When global ocean temperatures

are reduced to a minimum in 2070, the CO_2 emission growth from the oceans into the atmosphere is expected to be reduced.

5. Conclusion

This study investigates atmospheric CO_2 variability signatures. The study is based on a wavelet spectrum analysis of Atlantic CO_2 record for the period 1826 to 1960 and the Mauna Loa CO_2 records from 1959 to 2020. Together, the CO_2 records cover a total period of 200 years. The study has revealed that:

1. Atlantic CO_2 signature from 1826-1960 coincides with the Mauna Loa atmospheric CO_2 growth variability signature, the global sea surface temperature variability signature, and the lunar nodal tide variability signature. This is strong evidence of a lunar forced atmospheric CO_2 variations.
2. Atmospheric CO_2 variations have a maximum growth rate when global sea surface temperature variations have a maximum state. The $\pi/2$ (rad) phase lag between global sea temperature variations and atmospheric CO_2 variations, reveals that atmospheric CO2 variations are controlled by global sea temperature variations.
3. The CO_2 variability signature coincides with the lunar nodal tide signature. The lunar nodal tide spectrum reveals a chain of events from a lunar nodal tide variation to global sea surface temperature variations and atmospheric CO2 variations.
4. A lunar nodal tide spectrum in atmospheric CO_2 growth reveals that CO_2 is not controllable.

Global sea temperature variability has lunar forced periods up to 446 years and solar forced periods up to 4450 years (Yndestad 2022). The same solar forced periods and lunar forced periods are expected to be revealed in longer CO_2 time series.

Table 1. Identified signature of atmospheric Mauna Loa CO_2 growth, atmospheric Atlantic CO_2, Global Sea surface temperature and lunar nodal tide periods.

	Global Sea Surface temperature signature (SST)
Stationary SST periods (yr.)	T_{sst} = [9, 18, 28, 29, 37, 46, 57, 64, 74] (yr.)
Lunar nodal periods	$T_{ln}/2$ = [9.3, 18.6, 27.9, 37.2, 46.5, 55.8, 65.1, 74.4] (yr.)
Wsst(s, min/max/0, t)	[(-2.2, 1860), (-0, 1872), (2.2, 1883), (+0, 1897) (-3.1, 1912), (-0, 1927), (3.0, 1943), (+0, 1960), (-3.9, 1977), (-0, 1993), (5.1, 2008)]
	Mauna Loa CO_2 growth signature (dCO_2m/dt) 1959-2020
Stationary periods	$T_{co2\text{-}m}$ = [3, 9, 332] (yr.)
Lunar nodal periods	T_{ln} = [1/3, 1, 2, 3]18.61/2 = [3.1, 9.3, 18.6, 27.9] (yr.).
$W_{co2\text{-}m}$(s, min/max/0, t)	[(-1.64, 1965), (-0.0, 1973), (1.8, 1980), (+0.0, 1988), (-1.2, 1995), (-0, 2004), (2.5, 2013)]
	Atlantic CO_2 signature 1826-2020
Stationary periods:	$T_{co2\text{-}a}$ = [9, 18, 29, 39, 47, 64] (yr.)
Lunar nodal periods	T_{ln} = [1, 2, 3, 4, 5, 7]18.6/2 = [9, 18.6, 27.9, 37.2, 46.5, 65.1] (yr.)
$W_{co2\text{-}a}$(s, min/max/0, t)	[(1.6, 1831), (+0, 1839), (-2.0, 1846), (-0.0, 1852), (2.4, 1860), (+0.0, 1868), (-3.3. 1879), (-0.0, 1889), (2.6, 1898), (+0.0, 1907), (-3.5, 1919), (-0.0, 1929), (2.5, 1940)]
$W_{co2\text{-}a}$(s=37.2, min/max/0, t)	[(min, 1811), (max, 1829), (min, 1848), (max, 1866), (min, 1884), (max,1903), (min, 1922), (max, 1940), (min, 1959), (-0, 1968), (max, 1977), (+0, 1986), (min, 1996)… (-0, 2005), (max, 2014), (+0, 2023), (min, 2033)].
$W_{co2\text{-}a}$(s= 93.0, min/max/0, t)	[(6.0, 1845), (+0.0, 1868), (-7.0, 1895), (-0.0, 1921), (5.8, 1940), (+0, 1963), (min, 1986), (-0, 2009), (max, 2033), (+0, 2056)].
$W_{co2\text{-}a}$(s = 74.4, min/max, t)	[(max, 1866), (min, 1902), (max, 1940), (min, 1977), (max, 2014)]

Nomenclature

Atlantic CO_2 wavelet spectrum: $W_{co2\text{-}a}(s, t)$
Atlantic CO_2 wavelet autocorrelation spectrum: $WA_{co2\text{-}a}(R, T_{co2\text{-}a})$
Atlantic CO_2 stationary periods: $T_{co2\text{-}a}$
Cycle period spectrum: $T = [T_1, T_2, T_3 \ldots T_n]$
Coincidence cycle periods: $A*T_1 = B*T_2$
Global Sea Surface temperature: SST
Global Sea Surface temperature period spectrum: T_{sst}
Global Sea Surface temperature wavelet spectrum: $W_{sst}(s, t)$
Global Sea Surface temperature wavelet spectrum: $W_{sst}(s, t)$
Lunar nodal cycle periods: T_{ln}
Mauna Loa CO_2 stationary periods: $T_{co2\text{-}m}$
Mauna Loa CO_2 growth rate: $dCO_2(t)/dt$
Mauna Loa CO_2 wavelet autocorrelation spectrum: $WA_{aco2\text{-}m}(R, T_{co2\text{-}m})$

References

Ahn Jinho, Brook Logan Mitchell, Rosen Julia, McConnell Joseph R.. Taylor Kendrick, Etheridge David, and Rubino Mauro, 2012: *Atmospheric CO2 over the last 1000 years: A high-resolution record from the West Antarctic Ice Sheeet (WAIS) Divide ice core*, Global Biochemical Cycles, Vol. 26, Issue 2. https://doi.org/10.1029/2011GB004247

Anderson Thomas R., Hawkins Ed, Jones Philip D., 2016*: CO_2, the greenhouse effect and global warming: from the pioneering work of Arrhenius and Callendar to today's Earth System Models,* Endeavour, Volume 40, Issue 3, 2016, Pages 178-187, ISSN 0160-9327, https://doi.org/10.1016/j.endeavour.2016.07.002.

Beck Ernst-Georg, 2007: *180 Years of Atmospheric Co2 Gas Analysis by Chemical Methods.* Research Article. Energy & Environment, First Published March 1, 2007. https://doi.org/10.1260/095830507780682147.

Beck Ernst-Georg, 2008a: *50 Years of Continuous Measurement of Co2 On Mauna Loa,* Energy & Environment Vol 19 No 7. https://doi.org/10.1260/095830508786238288 Energy & Environment 19(7):1017-1028.

Beck Ernst-Georg, 2008b*: Evidence of variability of atmospheric CO2 concentration during the 20th century*. (discussion paper, May 2008). https://web.archive.org/web/20161201060229/http://www.biomind.de/realCO2/literature/evidence-var-corrRSCb.pdf

Beck Ernst-Georg, February 2010: *Reconstruction of Atmospheric CO_2 Background Levels since 1826 from direct measurements near ground.* Institute Biology III, University of Freiburg (personal communication).

Beck, Ernst-Georg, 2022*: Reconstruction of Atmospheric CO2 Background Levels since 1826 from Direct Measurements near Ground.* Science of Climate Change, 2, 148-211. https://doi.org/10.53234/scc202112/16

Daubechies, I. 1992: *Ten Lectures of Wavelet.* SIAM J. Math. Anal. 24, 499–519.

Gruber Nicolas, Gloor Manuel, Mikaloff Fletcher Sara E., Doney Scott C., Dutkiewicz Stephanie, Follows Michael J., Gerber Markus, Jacobson Andrew R., Joos Fortunat, Lindsay Keith, Menemenlis Dimitris, Mouchet Anne, Müller Simon A., Sarmiento Jorge L., and Takahashi Taro, 2009*: Oceanic Sources, Sinks, and Transport of Atmospheric CO_2.* Global Biogeochemical Cycles, 23, GB1005. https://doi.org/10.1029/2008GB003349

Humlum Ole, Stordahl Kjell, and Solheim Jan-Erik., 2013: *The Phase Relation Between Atmospheric Carbon Dioxide and Global Temperature*. Global and Planetary Change, Vo100, 51-69. https://doi.org/10.1016/j.gloplacha.2012.08.008.

Keeling C.D., Bacastow R.B., Bainbridge A.E., Ekdahl C.A., Guenther P.R., and Waterman L.S., 1976*: Atmospheric carbon dioxide variations at Mauna Loa Observatory, Hawaii,* Tellus, 28, 538-551. https://doi.org/10.1111/j.2153-3490.1976.tb00701.x

Keeling Ralph F, 2007: *Comment on "180 Years of Atmospheric Co2 Gas Analysis by Chemical Methods" by Ernst-Georg Beck.* Energy and Environment, 18(2), 259–282. https://www.jstor.org/stable/44397310.

Krajick Kevin, 2019: *Taro Takahashi, Who Uncovered Key Links Between Oceans and Climate. Traced Flows of Carbon Dioxide Across the Planet*. Columbia Climate School, Press Release, December 4. https://news.climate.columbia.edu/2019/12/04/taro-takahashi-who-uncovered-link-of-oceans-to-climate/.

Kunzig Robert and Broecker Wallace, 2008: *Fixing Climate*. Profile books ltd. London ISBN 987 1 84668 860 7.

Massen, Francis and Beck, Ernst-Georg, 2011: *Accurate Estimation of CO2 Background Level from Near Ground Measurements at Non-Mixed Environments.* In book: *The Economic, Social and Political Elements of Climate Change.* Edition: Climate Change Management. Chapter: 31. Publisher: Springer. Editor: Walter Leal Filho. https://doi.org/10.1007/978-3-642-14776-0. https://www.researchgate.net/publication/234004309_Accurate_Estimation_of_CO2_Background_Level_from_Near_Ground_Measurements_at_Non-Mixed_Environments

MATLAB 2020: MATLAB. *Wavelet Toolbox. Users Guide.* Portola Valley, CA, USA: The Math Works Inc.

Meiyer Harro A.J., 2007: *Comment on "180 Years of Atmospheric Co_2 Gas Analysis by Chemical Methods" by Ernst-Georg Beck:* Energy & Environment, 18(2), 2007. https://doi.org/10.1260/0958-305X.18.5.635.

Tansinez Pieter P., Fung Y. and Takahahi Taro, 1990: *Observational Constrains on the Global Atmospheric CO_2 Budget*. Science, Vol 247, No. 4949, 1431-1438. https://doi.org/10.1126/science.247.4949.1431.

Thoning K.W., Tans P.P. and Komhyr, W.D. *1989: Atmospheric Carbon Dioxide at Mauna Loa Observatory 2. Analysis of The NOAA GMCC Data, 1974-1985, J. Geophys. Research,* vol. 94, 8549-8565. https://doi.org/10.1029/JD094iD06p08549

Yndestad, H., Turrell, W. R., and Ozhigin, V., 2008: *Lunar Nodal Tide Effects on Variability of Sea Level, Temperature, and Salinity in the Faroe-Shetland Channel and the Barents Sea.* Deep Sea Res. Oceanographic Res. Pap. 55 (10), 1201–1217. https://doi.org/10.1016/j.dsr.2008.06.003.

Yndestad Harald, 2022: *Jovian Planets and Lunar Nodal Cycles in the Earth's Climate. Variability,* Frontiers in Astronomy and Space Sciences, 10 May. https://www.frontiersin.org/article/10.3389/fspas.2022.839794.

Conflict of Interest
No conflicts of interest are declared.

Author Contributions
This document is the author´s contribution.

Founding
This work has no founding.

Acknowledgments
The author thanks the editor Prof. Jan-Erik Solheim, guest editor Cand. Real. Stein Bergsmark. Valuable review comments from Prof. Ole Humlum, Cand. Real. Stein Bergsmark and Prof. Jan-Erik Solheim. Prof. Ole Henrik Ellestad and Prof. Jan-Erik Solheim for the many useful discussions of Beck´s work since 2009.